OF

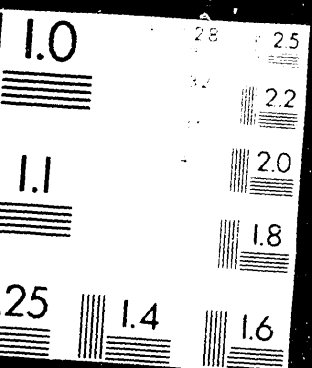

Conf-940115--16

ATMOSPHERIC AND DISPERSION MODELING IN AREAS OF HIGHLY COMPLEX TERRAIN EMPLOYING A FOUR-DIMENSIONAL DATA ASSIMILATION TECHNIQUE

by

J. D. Fast
B. L. O'Steen

Westinghouse Savannah River Company
Savannah River Site
Aiken, SC 29808

Publication Date: September 15, 1993

An extended abstract proposed for presentation at the
Eighth Joint Conferences on the Applications of Air Pollution Meteorology with the Air and Waste Management Association
Nashville, Tennessee
January 23-28, 1994

and for publication in the proceedings

DISCLAIMER

Available to DOE and DOE contractors from the Office of Scientific and Technical Information, P. O. Box 62, Oak Ridge, TN 37831; prices available from (615) 576-8401.

Available to the public from the National Technical Information Service, U. S. Department of Commerce, 5285 Port Royal Rd., Springfield, VA 22161

ATMOSPHERIC AND DISPERSION MODELING IN AREAS OF HIGHLY COMPLEX TERRAIN EMPLOYING A FOUR-DIMENSIONAL DATA ASSIMILATION TECHNIQUE

Jerome D. Fast, and B. Lance O'Steen

Savannah River Technology Center
Westinghouse Savannah River Company
Aiken, South Carolina

1. INTRODUCTION

The ability of mesoscale numerical models to incorporate high-resolution, asynoptic meteorological data will become increasingly important as additional operational and experimental remote sensing instrumentation networks (profilers, sodars, lidars, Doppler radars, etc.) become available during the 1990's. The near-continuous data available from these instrumentation networks and lower computational costs will make operational mesoscale numerical modeling more practical in the near future. Four-dimensional data assimilation (FDDA) techniques have been examined to (1) improve the initial conditions of mesoscale forecast models and (2) create high-quality four-dimensional mesoscale analysis fields. Several FDDA techniques have been developed recently to incorporate asynoptic observational data into atmospheric model forecasts (Harms et al. 1992). One of those techniques is Newtonian relaxation, in which the model variables are gradually driven toward the observations by extra forcing terms in the governing equations.

In this study, Newtonian relaxation is incorporated into a mesoscale atmospheric model and evaluated using meteorological and tracer data taken during the U. S. Department of Energy's (DOE) 1991 Atmospheric Studies in COmplex Terrain (ASCOT) field study along the Front Range of the Rockies in Colorado. The objectives of this study are (1) determine the ability of the model to predict small-scale circulations influenced by terrain, such as drainage flows, and (2) assess the impact of continuous data assimilation on the atmospheric and dispersion calculations. In contrast to a previous study (Fast and O'Steen 1992ab) in which the smallest horizontal grid spacing was 1 km, data assimilation is applied in this study to domains with a horizontal grid spacing as small as 330 m.

2. 1991 ASCOT FIELD EXPERIMENTS

The 1991 ASCOT field experimental study was conducted in an effort to better understand local circulations along Colorado's Front Range in the vicinity of Rocky Flats. It was conducted between January 28 and February 8 and focused on the nocturnal, locally generated flows from the canyons and off the slopes along the Front Range and their effect on transport and diffusion in the area. Intensive measurements were made by the ASCOT participants during eight nighttime periods and tracer (SF_6) experiments were performed in the area by Rocky Flats Plant personnel for four of those nights. Various instrumentation platforms were deployed in the area, which included meteorological towers, tethersondes, minisodars, a rawinsonde, an airsonde, and a Doppler lidar, with most of the instrumentation located just west of Rocky Flats Plant at the base of Coal Creek Canyon. Figures 1 and 2 depict the locations of the meteorological observations in the vicinity of Rocky Flats, including those from the NOAA/Forecast System Laboratory (FSL) mesonet and the 1991 Winter Icing and Storms Project (WISP).

The numerical simulations in this study focused on the second ASCOT field experiment during the evening of February 4 - 5. This particular period was chosen because of the well-developed drainage flows and a tracer experiment which was conducted that evening.

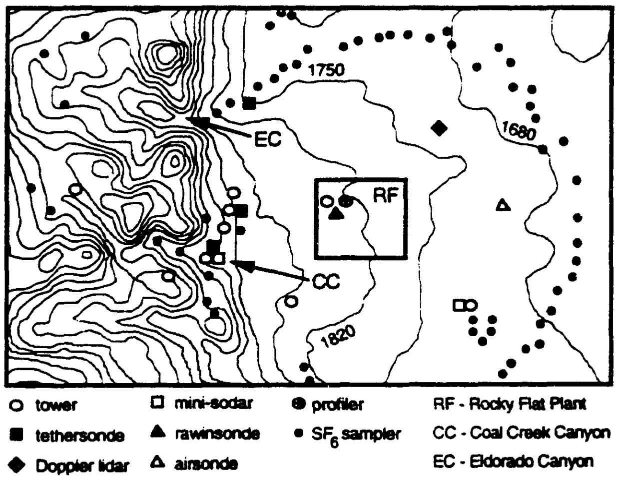

Fig. 1 Topography employed by RAMS on grid 4 and the locations of meteorological instrumentation and SF_6 samplers during the evening of Feb. 4 - 5

Corresponding author address: Jerome D. Fast, Westinghouse Savannah River Company, Building 773A, A1013, Aiken, SC, 29808.

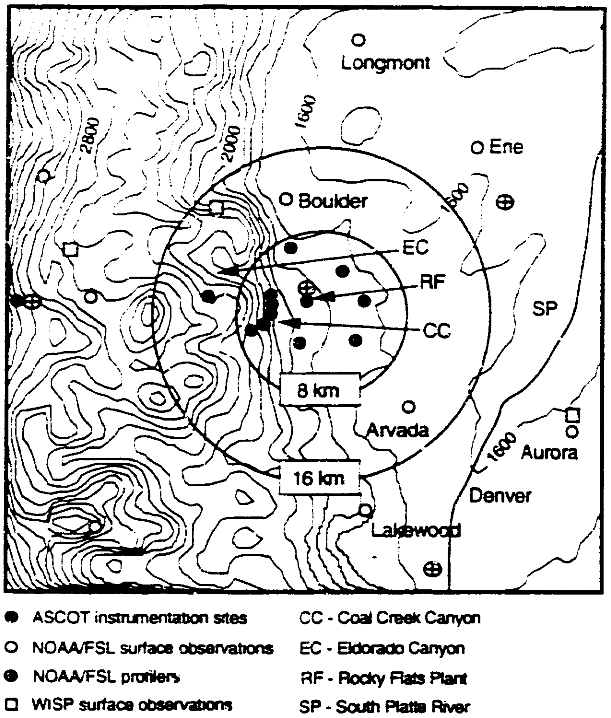

Fig. 2 Same as Fig. 1, except for grid 3 and approximate locations of SF_6 samplers depicted as concentric circles of radius 8 and 16 km

3. MODEL DESCRIPTION

3.1 *Atmospheric Model*

The Regional Atmospheric Modeling System (RAMS) developed at Colorado State University is a three-dimensional, primitive equation model that employs a terrain-following vertical coordinate system. A detailed description of the model equations and the numerical solution scheme is given elsewhere (Pielke et al. 1992). Version 2c of RAMS is used with a nested grid configuration; the outermost domain encompasses most of Colorado and southern Wyoming and three nested grids are centered over the vicinity of Rocky Flats. The characteristics of the nested grids are described in Table 1. Each domain has a vertical grid spacing of 26 m at the surface that gradually increases to 1000 m near the model top 16 km above ground level. The topography employed by the model for the two innermost nested grids (domains 3 and 4) are depicted in Figs. 1 and 2 along with some of the significant features in the area.

Version 2c of RAMS employs a first-order turbulence closure scheme based on the deformation of the flow field. A second-order turbulence closure scheme (Mellor and Yamada 1982) is incorporated into this version of RAMS for the simulations in this study. Heterogeneous vegetation characteristics are employed in the model to more accurately represent the fluxes of heat and momentum at the surface. The vegetation type in the Front Range area is derived from the U. S. Geological Survey (USGS) Advanced Very High Resolution Radiometer (AVHRR) imagery that is reclassified and interpolated to the RAMS grids (Finley and Pielke 1993).

Grid Characteristics	Domain			
	1	2	3	4
# E/W nodes	27	38	50	78
# N/S nodes	27	42	42	50
# vertical nodes	32	32	32	32
Δx, Δy (km)	21.12	5.28	1.32	0.33
time step (s)	20.0	10.0	5.0	2.5

Table 1. Characteristics of the nested grids employed by RAMS

3.2 *Initialization*

An isentropic analysis package is used to generate the initial conditions for RAMS for the numerical experiments in this study. The initial conditions are based on the large-scale NMC analysis, and upper-air and surface observations at 05 MST (12 UTC), Feb. 4, 1991. The model is initialized 15 hours before the release of the tracer at 20 MST so that a realistic boundary layer will evolve during the daytime.

3.3 *Four-Dimensional Data Assimilation*

A Newtonian (nudging) technique is incorporated in RAMS to bring the prognostic variables into closer agreement with the high-resolution data taken during the ASCOT experiment. In this technique, a tendency term is added to the governing equations of the form:

$$-G\,W(x,y,z)\,W(t)\,(V_{obs} - V_{mdl}) \qquad (1)$$

where G is the relaxation coefficient, W(x,y,z) the spatial weighting function, W(t) the temporal weighting function, V_{obs} the observed variable analyzed at a given grid point, and V_{mdl} the model variable at a given grid point. Any observed quantity that is also a prognostic variable can be employed in Eq. (1); however, V is either u or v for the simulations in this study.

Data is interpolated to the model grid at each observation time by a optimal interpolation method to obtain V_{obs}. The spatial weighting function, W(x,y,z), is based on the estimation variance of the interpolated data obtained from this method. If an observation is located precisely at a model grid point, W(x,y,z) = 1, and if a model point is sufficiently distant from the observation location, W(x,y,z) = 0; otherwise, the weight varies between 0 and 1 depending upon the spatial distribution and number of observations. The temporal weight varies linearly in time between 0 and 1 (Stauffer and Seaman 1990) and the value of G in this study is 0.005.

One advantage of Newtonian relaxation is that it is conceptually simple and computationally inexpensive. Newtonian relaxation is a practical FDDA method for applications in regions of complex terrain due to extensive computational requirements of state-of-the-art variational techniques, such as the adjoint method. Another advantage is that continuous FDDA produces a flow field that is a combination of the predicted and observed variables when and where the observations may occur. In data sparse regions, only the model governing equations are used to predict the flow field. Theoretically, continuous FDDA should be superior to mass-consistent diagnostic models that simply interpolate the wind field in three dimensions into data sparse regions. Spatial and temporal interpolation techniques employed by these diagnostic models may result in significant wind speed and direction errors, especially in highly complex terrain. Data assimilation also allows a prognostic model to "spin-up" to accurate, complex circulations in a shorter period of time. Currently, prognostic mesoscale models often employ horizontally homogeneous initial conditions for simulations in complex terrain; realistic terrain-induced circulations are obtained only after prolonged "spin-up" periods. While horizontally homogeneous initial conditions maybe adequate in certain situations, three-dimensional, synoptic or mesoscale influences that normally exist are neglected.

The disadvantages of Newtonian relaxation is that the relaxation coefficient, G, is assigned arbitrarily and the assimilation of local or unrepresentative components can occur (i.e., microscale observations may be spread over a relatively large area). For instance, the influence of an observation at a valley floor location can be spread up the valley walls. In nocturnal periods, this may result in a winds not flowing directly down the slope of the valley walls. To reduce the impact of this problem, the spatial weighting function, W(x,y,z), in this study approaches zero 2 km from an observation location on the innermost nested grid. The optimal interpolation method employed by the FDDA technique can also be modified to include non-spherical estimation variances for W(x,y,z). This would enable the user to weight observations based on known preferential wind directions for specific locations; however, this is not performed in this study.

3.4 *Dispersion Model*

A Lagrangian Particle Dispersion Model (LPDM), described by McNider et al. (1988), is used in this study to simulate the dispersion in complex terrain around Rocky Flats. The mean wind components produced by RAMS are used as inputs to LPDM. The turbulent velocity fluctuation of the non-buoyant tracer particles are determined by:

$$u_\alpha''(t+\Delta t) = u_\alpha''(t)\, R_\alpha(\Delta t) + u_\alpha'''(t) \qquad (2)$$

where α is 1, 2, or 3, u_α'' the subgrid-scale velocity component, R_α the autocorrelation coefficient, and u_α''' the random turbulent component independent of u_α''. A drift correction term is added to Eq. (2) for $\alpha = 3$. This equation is the finite difference analog to the Langevin stochastic differential equation. LPDM has been modified to (1) ensure that the turbulent velocity statistics are consistent with the second-order closure applied in RAMS, (2) include effect of vertical inhomogeneity in the second-order moments (drift corrections) in all the random velocity components, and (3) calculate instantaneous and time-averaged concentrations at arbitrary points.

4. NUMERICAL RESULTS

4.1 *Experimental Design*

Three simulations were performed to examine the effect of data assimilation on the forecasts made by RAMS:

case 1	static, horizontally homogeneous initial conditions based only on the temperature and moisture profile (no winds) obtained from the Denver sounding at 05 MST, Feb. 4
case 2	static, inhomogeneous initial conditions obtained from the large-scale NMC analysis at 05 MST, Feb. 4
case 3	same as case 2, except continuous FDDA was employed on all the nested grids

Case 1 is used to isolate the nocturnal slope flows without the complications of synoptic flow that is included in case 2. The isentropic analysis package generates the initial conditions for RAMS for cases 2 and 3. Case 3 is used to evaluate the impact of FDDA on the model results and to produce high-quality mesoscale analysis fields for the dispersion calculations. Surface and upper-air observations from both the 1991 ASCOT field experiment and the NOAA/FSL and WISP mesonets (meteorological towers [10], surface observations [52], mini-sodars [2], rawinsonde [1], airsonde [1], tethersondes [3], and profilers [5]) are incorporated into the analysis fields created by FDDA.

4.2 *Meteorological Fields*

The lowest model level wind fields on grid 4 for cases 2 and 3 at 20 MST, Feb. 4 are displayed in Figs. 3a and 3b. Observations near the surface at the same time are shown in Fig. 3c. Case 2 predicts a strong jet exiting Eldorado Canyon, with wind speeds up to 9 m s^{-1}. The jet flows out of the canyon over the plains, producing strong northwesterly winds over Rocky Flats. A somewhat weaker jet exits Coal Creek Canyon with wind speeds approaching 5 m s^{-1}. It is much smaller in extent because the canyon itself is narrower and shorter than Eldorado Canyon. The Eldorado Canyon jet is strong enough to push the Coal Creek jet to the south. The flow field at this time for case 1 (without synoptic forcing) is similar to Fig. 3a, except that the wind speeds are lower by 1 - 2 m s^{-1} and the wind directions are more westerly over the Rocky Flats vicinity (not shown). This indicates that the synoptic forcing has a significant effect on the speed and direction of the drainage flows predicted by RAMS during this evening.

As shown in Fig. 3b, the wind speeds are reduced significantly throughout most of the domain when FDDA is employed. The Coal Creek Canyon jet does not extend as far east as case 2, but its influence spreads over more of the Rocky Flats area since the maximum wind speed of the Eldorado Canyon jet has also been reduced. The FDDA procedure incorporates the observations shown in Fig. 3c, and the wind directions in case 3 are in better agreement with the observations as expected. The jet exiting Eldorado Canyon is also better simulated in case 3 than case 2 when compared to the tethersonde data at 21 MST, (not shown). The jet produced in case 2 is too strong and the wind speed maximum is 250 m above the observed maximum.

To demonstrate the effect of FDDA on the flow field at larger horizontal scales, the lowest model level wind field at 20 MST for grid 2, along with the observations near the surface is shown in Fig. 4. In case 2, RAMS is able to forecast a drainage flow down the slopes of the foothills that merges with the drainage flow along the S. Platte River basin that is qualitatively similar with the observed wind field. However, there is a large area of relatively weak winds from Denver to the middle of the S. Platte River basin that is not produced by RAMS. Case 3 is able reproduce more of the observed features including the calm winds in the middle of the S. Platte River basin, the strong southerly flows down the Palmer Ridge, and the northerly flows down the Cheyenne Ridge as seen in Fig. 6b

All of the simulations appear to produce a large amount of spatial and temporal variability in the wind field that wss observed during the evening of Feb. 4 - 5; but, the drainage flow in the early evening hours is nearly steady in case 1. The model indicates that both the canyon jets can have an impact on the flow field over Rocky Flats, as seen in Fig. 3. Small changes in the strength of either of these jets can have a significant impact on the drainage flow over Rocky Flats.

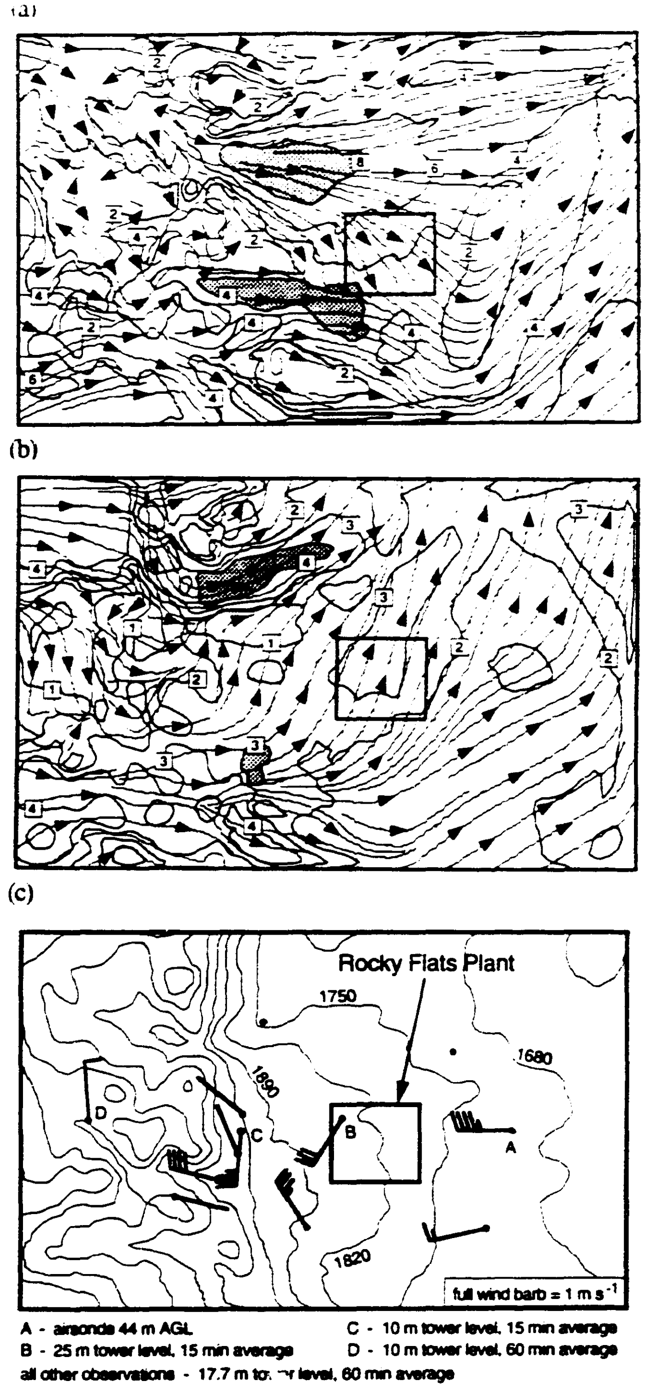

Fig. 3 Predicted wind field 26 m AGL for grid 4 at 20 MST for (a) case 2 and (b) case 3, and (c) the observed wind field near the surface

4.3 *Dispersion*

The high-resolution wind and turbulence fields determined by RAMS from case 3 were also be used to determine tracer transport around Rocky Flats during the evening of Feb. 4 and 5. An example of the hourly averaged surface concentrations is shown in Figs. 5 and 6. Between 02 - 03 MST, the plume has advected downwind beyond the 16 km sampler arc, following the terrain slope down to the S. Platte River (Fig. 5). At

(a)

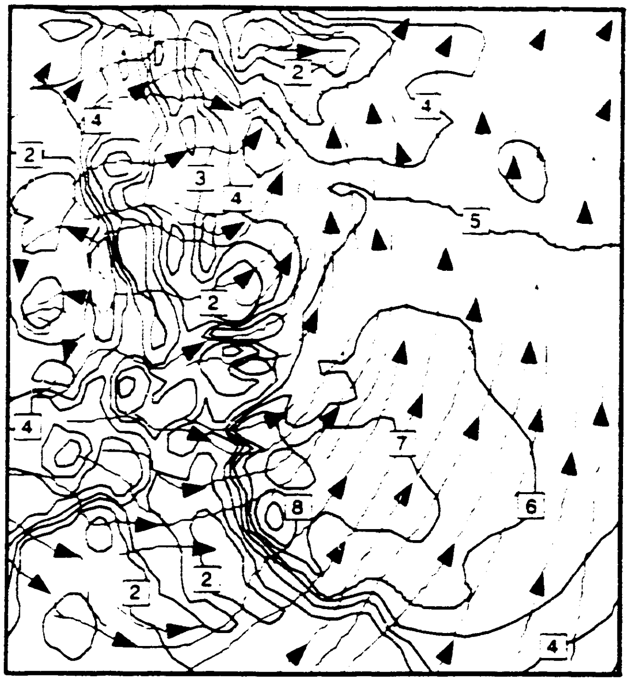

(b)

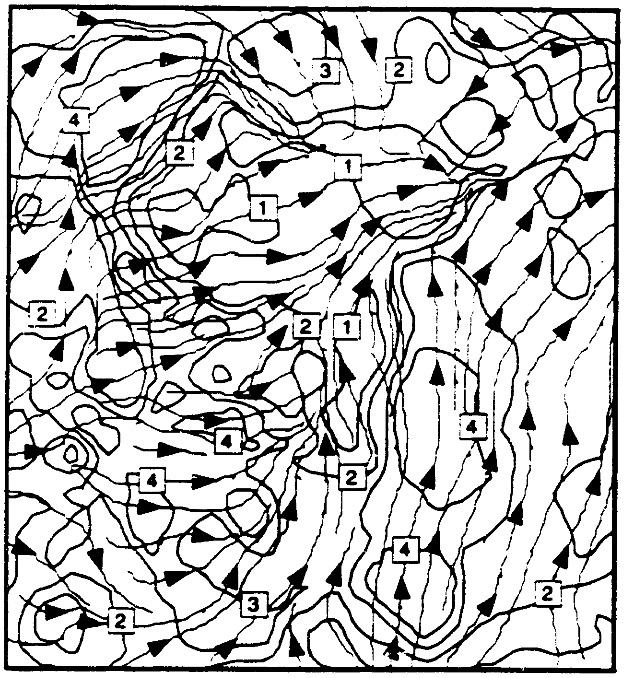

Fig. 4 Predicted wind field 26 m AGL for grid 2 at 20 MST for (a) case 2 and (b) case 3, and (c) the observed wind field near the surface

this time, the surface concentrations are too high on the inner arc and too low on the outer arc (Fig. 6). The model does predict two plume peaks on the inner arc, but they are not as distinct as the observed peaks.

(c)

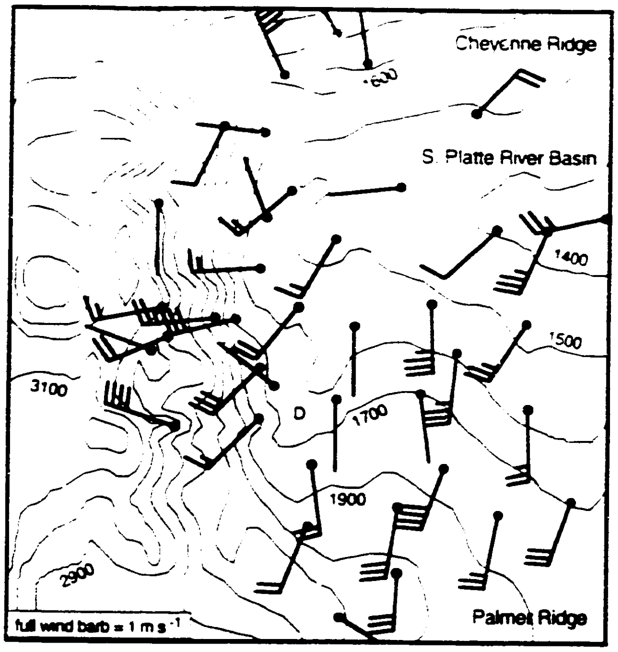

all observations - 10 m AGL, 15 min average

There are periods in which the performance of RAMS and LPDM is better; however, there are also periods when surface concentrations are underpredicted. This occurs, in part, because the maximum concentration of the simulated plume was located up to 100 m above the ground at times.

Another way to compare the dispersion calculation with the observations is to examine the concentrations summed over the entire evening. This is especially useful for radiological releases in which a dose must to be computed. Figure 7 shows the footprint of the plume and Fig. 8 compares the observed and simulated integrated concentrations. The model does quite well in determining the path of the plume, except at the north end of the outer arc where some very low concentrations are missed.

5. CONCLUSIONS

The results of this study indicate that the current data assimilation technique can have a positive impact on the mesoscale flow fields; however, care must be taken in its application to grids of relatively fine horizontal resolution. Continuous FDDA is a useful tool in producing high-resolution mesoscale analysis fields that can be used to (1) create a better initial conditions for mesoscale atmospheric models and (2) drive transport models for dispersion studies. While RAMS is capable of predicting the qualitative flow during this evening, additional experiments need to be performed to improve the prognostic forecasts made by RAMS and refine the FDDA procedure so that the overall errors are reduced even further.

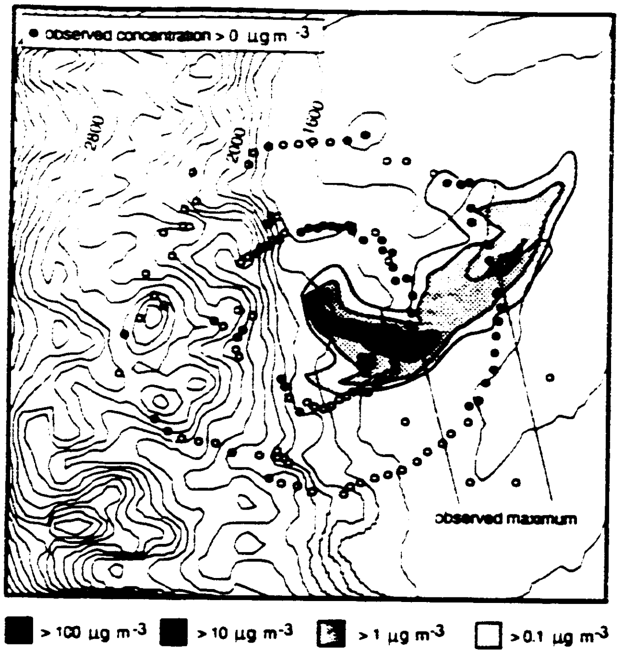

Fig. 5 Hourly-averaged concentration determined by LPDM on grid 3 between 02 - 03 MST

Despite the fact that a great deal of computational time is necessary in executing RAMS and LPDM in the configuration employed in this study, recent advances in workstations is making applications such as this more practical. As the speed of these machines increase in the next few years, it will become feasible to employ prognostic, three-dimensional mesoscale/transport models to routinely predict atmospheric dispersion of pollutants, even in highly complex terrain. For example, the version of RAMS in this study could be run in a "nowcasting" mode that would continually assimilate local and regional observations as soon as they become available. The atmospheric physics in the model would be used to determine the wind field where no observations are available. The three-dimensional flow fields, such as those in Figs. 3b and 4b, could be used as dynamic initial conditions for a model forecast. The output from this type of modeling system will have to be compared to existing diagnostic, mass-consistent models to determine whether the wind field and dispersion forecasts are significantly improved.

6. REFERENCES

Fast, J. D., and B. L. O'Steen, 1992a: Numerical simulation of the transport and diffusion during the Winter Validation Study along the Front Range. Preprints, *Tenth Symposium on Turbulence and Diffusion*, Portland, OR, Amer. Meteor. Soc. (J7) 167-170.

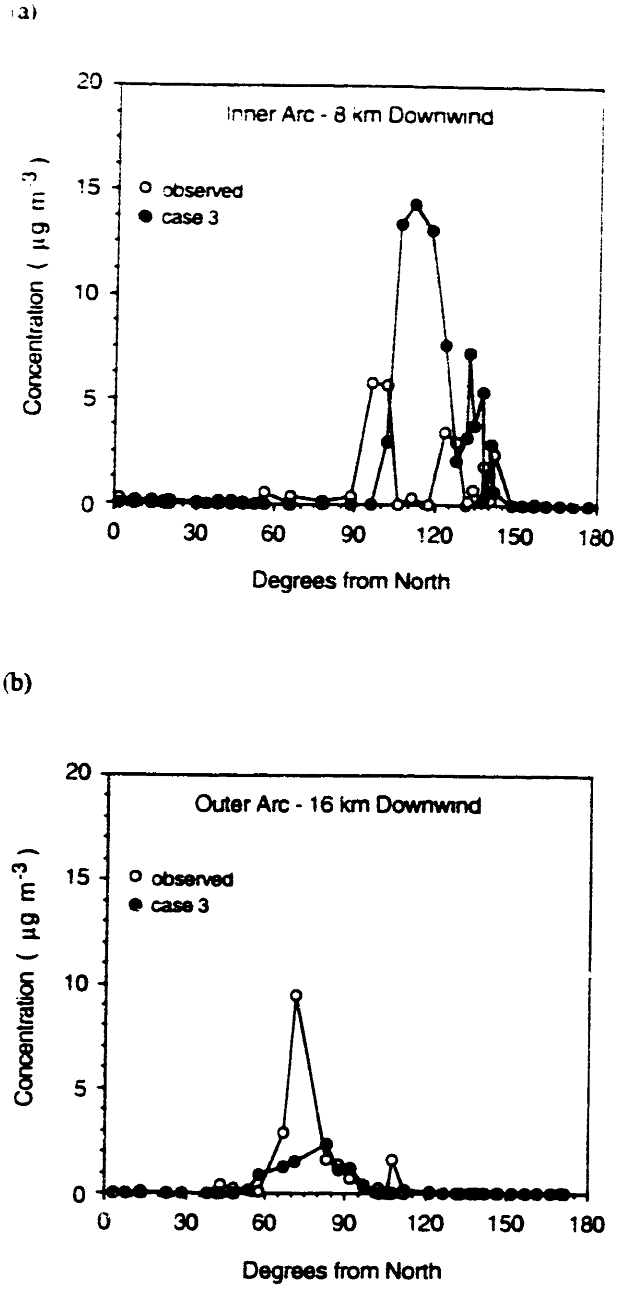

Fig. 6 Hourly-averaged concentration determined by LPDM on the (a) inner and (b) outer sampler arc between 02 - 03 MST

Fast, J. D., and B. L. O'Steen, 1992b: Use of the 1991 ASCOT field study data in a mesoscale model employing a four-dimensional data assimilation technique. Preprints, *Sixth Conference on Mountain Meteorology*, Portland, OR, Amer. Meteor. Soc., 249-255.

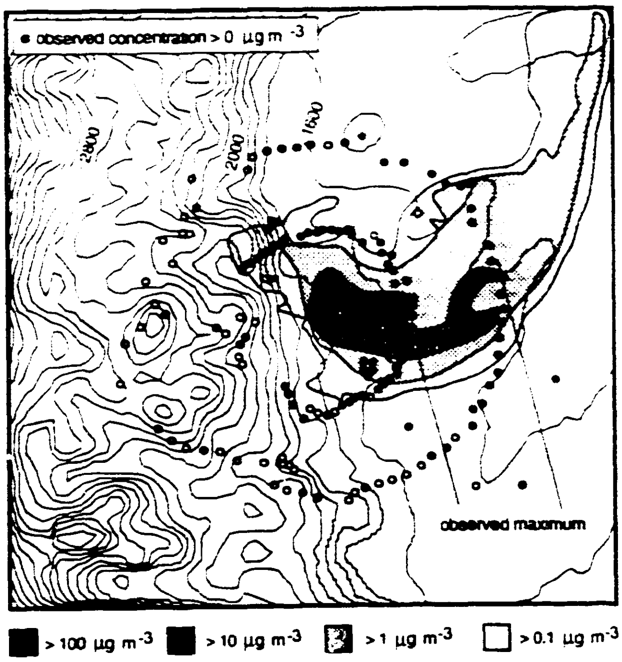

Fig. 7 Surface concentration determined by LPDM on grid 3 summed over the entire evening

Finley, C., and R. A. Pielke, 1993: Possible effects of land use variability on atmospheric mesoscale circulations and pollutant dispersion. Preprints, ANS Topical Meeting on Environmental Transport and Dosimetry, Charleston, SC, Amer., Nuclear Soc., 7-10.

Harms, D. E., S. Raman, and R. V. Madala, 1992: An examination of four-dimensional data-assimilation techniques for numerical weather prediction. *Bull. Amer. Met. Soc.*, **73**, 425-440.

McNider, R. T., M. D. Moran, and R. A. Pielke, 1988: Influence of diurnal and inertial boundary-layer oscillations on long-range dispersion. *Atmos. Environ.*, **22**, 2445-2462.

Mellor, G. L, and T. Yamada, 1982: Development of a turbulence closure for geophysical fluid problems. *Reviews of Geophysics and Space Physics*, **20**, 851-875.

Pielke, R. A., W. R. Cotton, R. L. Walko, C. J. Tremback, W. A. Lyons, L. D. Grasso, M. E. Nicholls, M. D. Moran, D. A. Wesley, T. J. Lee, and J. H. Copeland, 1992: A comprehensive meteorological modeling system - RAMS. *Meteorology and Atmospheric Physics*, **49**, 69-91.

Stauffer, D. R., and N. L. Seaman, 1990: Use of four-dimensional data assimilation in a limited area mesoscale model. Part I: Experiments with synoptic-scale data. *Mon. Wea. Rev.*, **118**, 1250-1277.

Acknowledgments. This work was supported by the U. S. Department of Energy's ASCOT program through the Office of Health and Environmental Research (OHER).

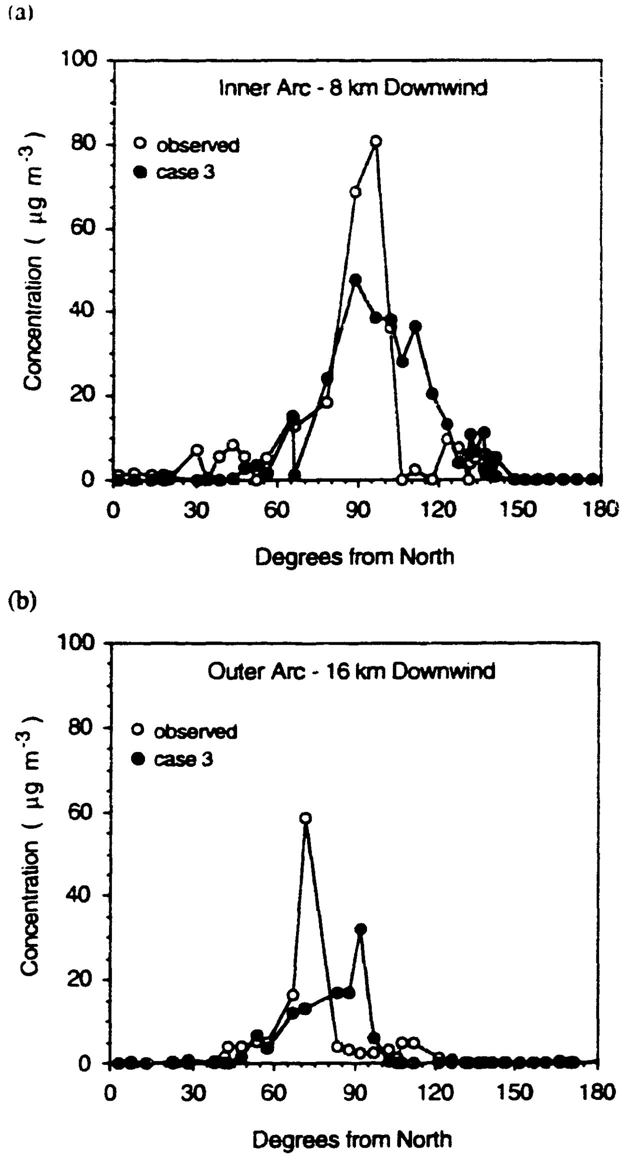

Fig. 8 Surface concentration determined by LPDM on the (a) inner and (b) outer sampler arc summed over the entire evening

DATE
FILMED
5/19/94

END